



Optimization of diesel engine characteristics using p-toluene sulfonic acid catalyst-based biodiesel from waste chicken fat oil

Muhammad Usman^{a,*}, Muhammad Abrar^a, Touqeer Ahmad^a, Fahid Riaz^{b,*},
Fahad Rehman^c, Nasir Hayat^a, Yasser Fouad^d, Fahed Javed^c, M.A. Mujtaba^a, M.A. Kalam^e

^a Department of Mechanical Engineering, University of Engineering and Technology, UET, Lahore 54890, Pakistan

^b College of Engineering, Abu Dhabi University, Abu Dhabi, United Arab Emirates

^c Microfluidics Research Group, Department of Chemical Engineering, COMSATS University Islamabad, Lahore Campus, Pakistan

^d Department of Applied Mechanical Engineering, College of Applied Engineering, Muzahimiyah Branch, King Saud University, P.O. Box 800, Riyadh 11421, Saudi Arabia

^e School of Civil and Environmental Engineering, FEIT, University of Technology Sydney, NSW 2007, Australia

ARTICLE INFO

Keywords:

Waste chicken fat
Biodiesel
Microbubble
Diesel engine
Performance characteristics
Emissions

ABSTRACT

Amidst rising global demand for sustainable energy substitutes and the complex hindrances connected with a full-scale shift to new technologies, internal combustion engines (ICEs) using biofuels like biodiesel are progressively acquiring a vital role. However, an immediate global focus is required for cost-effective and eco-friendly biodiesel production. The issues linked with the operating parameters of these ICEs mandate methodical optimization. The study utilized microbubble-mediated esterification with p-toluene sulfonic acid, achieving 89.9 % biodiesel conversion from waste chicken fat in 30 min. Waste chicken fat biodiesel (WCFB) met ASTM D6751 and EN-14214 standards, demonstrating its potential as an alternative fuel. A single-cylinder, direct-ignition engine was tested with WCFB blends (10 %, 20 %, 30 %, and 40 %) to assess performance and emissions in comparison to diesel fuel. Using response surface methodology, optimized conditions (14.2%WCFB and 1845 rpm) resulted in a 5.6 % increase in torque, 8.9 % more brake power, and a 7.7 % improvement in brake thermal efficiency, along with a 15.9 % reduction in brake-specific fuel consumption. Carbon monoxide emissions decreased by 4.6 %, while exhaust gas temperature and NO_x emissions increased by 10.9 % and 4 %, respectively. This study aligns with multiple sustainable development goals, contributing to a more sustainable and resilient future for the planet.

1. Introduction

There are 1.2 billion passenger automobiles and 380 million commercial vehicles in operation that are utilizing internal combustion engines (ICEs) for propulsion [1]. The registered motor vehicles only in Pakistan are projected to exceed 30 million by year 2025. In Pakistan, over 50 % of energy consumption relies on petroleum products like furnace oil, diesel fuels (DF), and gasoline. Road transport is the largest oil-consuming sector, with 46 % of export earnings spent on oil imports. ICEs using biofuels like biodiesel are gaining importance because of the rising need for sustainable energy solutions and the difficulties in complete transfer to new technology [2]. Therefore, immediate action is required for the optimization of these ICEs to address critical problems with their emissions, and performance [3].

The recognition of an affordable and easily accessible raw material for biodiesel synthesis is significant [4]. Sustainable development goals (SDGs), SDGs 7 (affordable and clean energy) and 13 (taking climate action), emphasize the need to switch to sustainable and clean energy, are exactly in line with this investigation [5]. The expense of raw materials accounts for 70–95 % of the total biodiesel synthesis cost [6]. Furthermore, the waste-to-energy production reduces emissions while supplying the world's energy needs [7]. Energy generated from garbage instead of fossil fuels reduces environmental harm and carbon dioxide (CO₂) emissions [8]. In comparison to feed stocks, the waste chicken fat (WCF) is an affordable feedstock, costing less than 120 USD ton⁻¹. It is also widely accessible around the world as biodegradable waste. For instance, roughly 115,500 tons of chicken fat are wasted each year in China, and 77,000 tons are wasted each year in India, respectively [9].

* Corresponding authors.

E-mail addresses: muhammadusman@uet.edu.pk (M. Usman), fahid.riaz@adu.ac.ae (F. Riaz).

<https://doi.org/10.1016/j.aej.2024.12.086>

Received 28 January 2023; Received in revised form 4 December 2024; Accepted 23 December 2024

Available online 26 December 2024

1110-0168/© 2024 The Author(s). Published by Elsevier B.V. on behalf of Faculty of Engineering, Alexandria University. This is an open access article under the CC BY-NC-ND license (<http://creativecommons.org/licenses/by-nc-nd/4.0/>).

Pakistan’s poultry sector is well-established and generates 1.26 % of the country’s gross domestic product (GDP) [10]. One million tons of manure are produced annually by more than 25,000 chicken farms [11]. A novel bionic flow-induced peristaltic reactor with high conversion rate is developed for efficient biofuel production from high-concentration fluids, achieving a conversion efficiency of 89.9 % at 10 s, significantly higher than traditional rigid tube reactors [12]. Due to its low cost and easy accessibility, there is a high potential to use it as a biodiesel feedstock. Furthermore, the current concern of Pakistan regarding waste management can be greatly improved.

The benefits can only be grasped if biodiesel is produced in a convenient, responsible (SDG 12), frugal, and eco-friendly manner (SDG 9) [13]. These SDGs promote sustainable industrial growth, ingenuity, and infrastructure for ecological sustainability and economic progress [14]. Furthermore, the prevalent technique for biodiesel synthesis, transesterification, involves a catalyst-mediated interaction between alcohol and high-density lipoprotein [15,16]. During biodiesel production, chicken fat undergoes alkaline catalysis saponification, which can be challenging due to the high content of Free Fatty Acids (FFAs). The saponification process can be reduced converting all FFAs into Fatty Acid Methyl Esters (FAMES) to increase the efficiency of biodiesel production. In addition, the process increases downstream separation costs [17]. Another restriction of acid catalysis is the development of equilibrium, which results in a reaction rate 4000 times slower than transesterification [18]. The primary reason for this constraint is that methanol from feedstock oil has a non-homogenous or low-homogenous character. The extent of close contact that occurs between the reactants is significantly reduced owing to the formation of a thin methyl group linked to a hydroxyl group (MeOH) layer. As a direct consequence of this, the rate of mass transfer is slowed down. The present study has utilized an innovative method that involves the infusion of methanol in the form of microbubbles to address the very concern.

Table 1 outlines the past investigations undertaken by several researchers who prepared biodiesel from WCF using various catalysts and examined its influence on engine emissions and efficiency. Zheng et al. conducted a study to compare diesel engine operating characteristics during high-load engine conditions using canola, soy, and yellow grease-derived pure biodiesel (B100) biodiesel fuels. The authors concluded that biodiesel possessing a cetane number (CN) comparable to diesel demonstrated relatively elevated NOx emissions [19]. Wei, L. et al. conducted research on the impact of biodiesel-n-butanol blends for diesel engine’s performance, combustion, and emissions. The study revealed lower levels of carbon monoxide (CO) and hydrocarbon (HC) emissions [20]. Behçet et al. produced chicken oil methyl ester from

inexpensive waste fish and chicken oils via transesterification. The fuels were employed in a diesel engine to ascertain the emissions trends. The biodiesel utilization reduced CO, HC, CO₂, and increased NOx emissions [21]. El-Shafay et al. produced chicken fat oil biodiesel via esterification and transesterification. Adding biodiesel in diesel fuel resulted in a 12 % reduction in CO emission [22].

However, Shudo et al.’s findings demonstrated that biodiesel-ethanol blends reduce NOx and smoke emissions while having significant impact on brake thermal efficiency (BTE) [23]. Dhana Raju, V. et al. achieved a decrease of 24.4 % in HC and a 16.9 % reduction in CO by combining a 20 % lemon peel oil blend with 10 % diethyl ether [24]. Aydin et al. noted that 20 % sunflower oil based biodiesel blend with 80 % diesel resulted in higher BTE and lower CO emissions values. In addition, increment in nitrogen oxides (NOx) emissions was also observed at lower engine speeds [25]. Chaurasiya, P.K. et al. achieved the lowest levels of CO₂ and smoke particles using 95 % of diesel fuel, diethyl ether and, n-butanol mixture with hydrogen supplementation of 5 % [26]. Elkelaywy et al. investigated sunflower-soybean oil methyl ester production via catalyzed transesterification. Response surface methodology (RSM) optimization yielded optimal values of BTE (13.66 %), HC (120.77 ppm), and NOx (234.89 ppm) emissions for 70 % biodiesel and diesel blend formation [27]. Upendra Rajak et al. evaluated compression ignition engine performance and emission indices using diesel and spirulina microalgae-based biodiesel (SMB) blends. The fuel blend (20 % by volume) depicted a reduction in brake torque, efficiency, and mechanical efficiency, while reducing NOx, smoke, and CO₂ emissions [28]. In lieu of the past studies, there exists a gap in the optimization of WCFB utilization in diesel engines. Table 1 displays the novelty of the present study where RSM is utilized by examining a more diverse set of outputs to optimize the engine that is powered with WCFB

The current study provides a multifaceted approach that incorporates innovative feedstock utilization and, microbubble-mediated mass transfer along with comprehensive optimization technique. The study offers an innovative solution to the related waste management issue by recycling waste chicken fat that would otherwise be discarded. Additionally, multiple SDGs are well-aligned with this strategy. Additionally, extending the study’s geographical scope outside Pakistan provides insightful information on the possible uses of waste-derived biodiesel in various areas with diverse waste management infrastructures and energy demands. This research is notable for its contribution to reaching multiple SDGs simultaneously and promoting a sustainable and resilient future for the entire planet.

Table 1
Summary of researchers’ work exploring different catalysts for the production of waste chicken fat biodiesel and examining its impact on engine performance and emissions.

Author	Catalyst		Performance				Emissions				Engine Optimization
	Esterification	Transesterification	Torque	BP	BSFC	BTE	EGT	CO	CO ₂	NOx	
Behçet et al. [21]	H ₂ SO ₄	NaOH	✓	✓	✓	✓	✓	✓	✓	✓	×
Barik and Vijayaraghavan [29]	H ₂ SO ₄	Na ₂ O ₃ Si	✓	✓	✓	✓	✓	✓	✓	✓	×
Ge et al. [17]	H ₂ SO ₄	CaO (eggshells)	✓	✓	✓	✓	✓	✓	✓	✓	×
Mohiddin et al. [30]	H ₂ SO ₄	NaOH	×	✓	✓	✓	×	×	×	×	×
Kirubakaran [31]	HCL	CaO (eggshells)	×	✓	✓	✓	×	✓	✓	✓	×
Şen et al. [32]	H ₂ SO ₄	KOH	✓	✓	✓	✓	×	✓	✓	✓	×
El-Shafay et al. [22]	H ₂ SO ₄	KOH	×	✓	✓	✓	✓	✓	✓	✓	×
Yi-Chia et al. [33]	H ₂ SO ₄	CaO (eggshells)	✓	✓	✓	✓	✓	✓	✓	✓	×
Wang et al. [34]	H ₂ SO ₄	KOH	×	✓	✓	×	✓	✓	×	✓	×
Kinnal et al. [35]	H ₂ SO ₄	NaOH	×	×	✓	✓	×	×	×	×	×
Present Study	PTSA (Single Step Esterification -Microbubbles Process)		✓	✓	✓	✓	✓	✓	✓	✓	✓

2. Materials and methods

This section elaborates on WCFB production, the outline of the experimental blueprint for engine testing, and engine optimization driven by RSM.

2.1. Biodiesel production

The production methodology is summarized in Fig. 1. WCF was gathered from a nearby slaughterhouse located on the periphery of Lahore, Pakistan. Tap water was used to cleanse it and eliminate blood and solid impurities to extract chicken fat oil (CFO). 5 kg of purified chicken fat was heated to 110 °C for six hours using an oven made of Bio-Base China. Whatman® grade 42 filter paper was used to separate the oil from the solid debris. The characteristics of the acquired CFO are outlined in Table 2.

The method for WCFB production involves the infusion of methanol as microbubbles for enhancing the rate of mass transfer during esterification processes [36,37]. Owing to reduced buoyancy, microbubbles linger longer in the liquid phase, aiding methanol-CFO mass transfer. The reaction rate is increased by their greater surface penetration and longer retention period. Larger bubbles might, however, develop as a result of clumping. Even so, the small size of microbubbles allows for a longer residence time in laminar flow, which leads to significant inner fusion and uniformity at a millisecond scale for microbubbles that are

Table 2
Chicken fat oil properties.

Property	Value
Viscosity (40°C)	44.2 mm ² /sec
FFA	7%
Acid Value (KOH/g)	13.9 mg
Density	925 kg/m ³

100 mm in size [38].

During the research, biodiesel production conditions were adopted based on the literature study [39]. This involves a molar ratio of 1–13.7, operating at 70 °C, for 30 min. The catalyst was loaded at 7 wt%, with a headspace ranging from 1 to 1.5 in. PTSA and CFO were first mixed for 45 min before being introduced to the reactor to start the esterification reaction in the presence of the catalyst PTSA. A temperature-controlled heating mantle was utilized to heat MeOH while vapor pressure was measured at 1.025 bar using the Bourdon gauge. MeOH vapors were introduced into the reactor as bubbles. The process halted once the necessary quantity of MeOH evaporated. The reaction mixture's temperature was observed and controlled during the process. At different time points, samples were collected and subjected to liquid-liquid extraction with heated ultrapure water. The mixture of samples and water resulted in the formation of two layers. The process involved repeated separation using a separation flask to ensure thorough isolation of glycerol and catalyst from the biodiesel layer. The specimens were

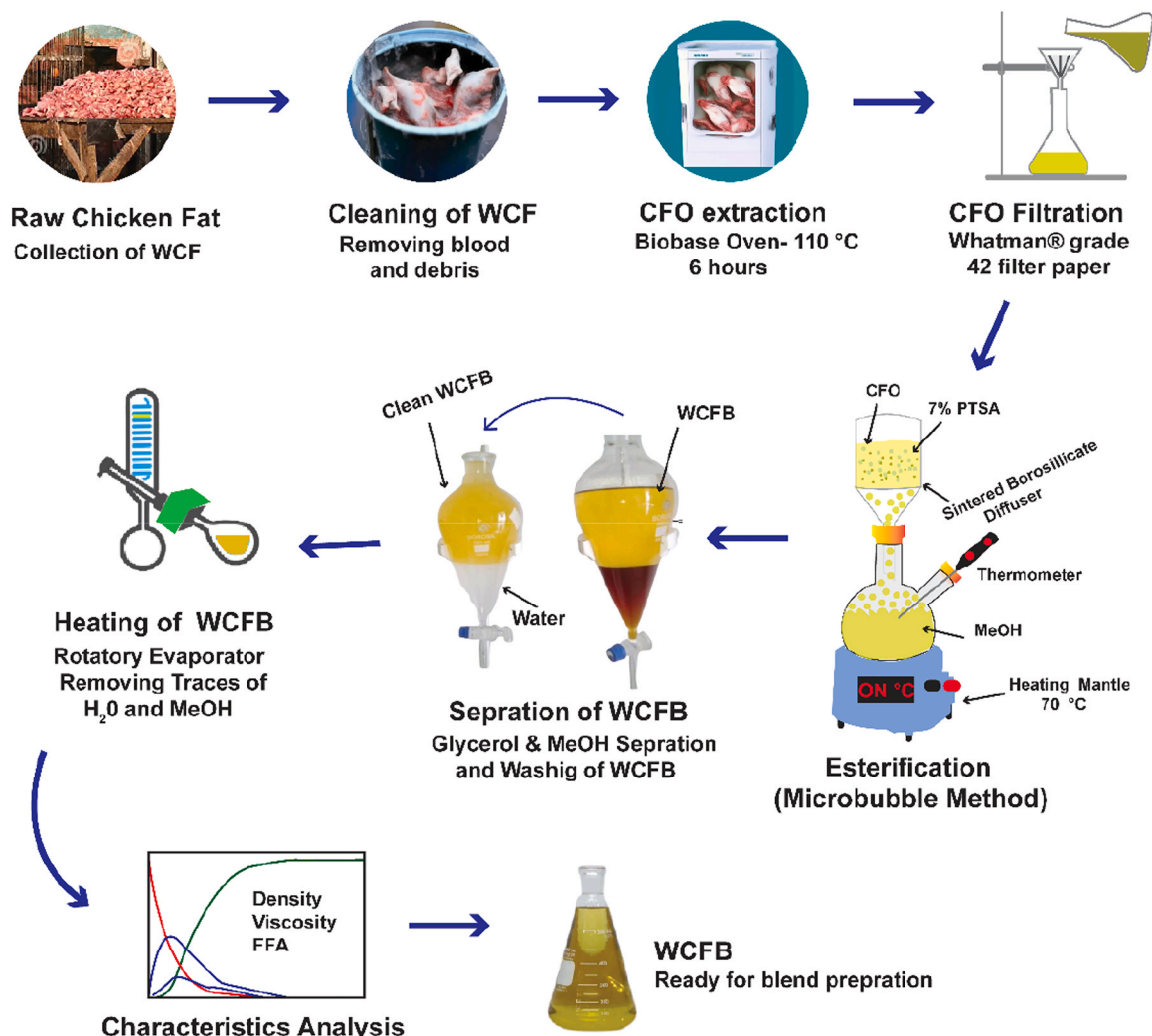


Fig. 1. The methodology for making waste chicken fat biodiesel through the microbubble esterification process.

dehydrated using a Buchi R-210 evaporator to eliminate any remaining trace amounts of MeOH. A Shimadzu system was utilized to direct GC-FID analysis. Table 3 outlines the primary parameters considered in the analyses.

2.2. Experimental strategy for engine testing

A Lombardini - 15 LD 315 single-cylinder, 4-stroke, direct injection, air-cooled diesel engine was utilized for testing. Table 5 outlines the technical features of the engine. The blend composition has a significant impact on the results of engine testing. Therefore, reasoned selection for the appropriate blend composition is required. The study investigated four fuel blends initially: WCFB10 (10 % CFO biodiesel - 90 % DF), WCFB20 (20 % CFO biodiesel - 80 % DF), WCFB30 (30 % CFO biodiesel - 70 % DF), and WCFB40 (40 % CFO biodiesel - 60 % DF). The original test rig is presented in Fig. 2.

Fig. 3 depicts the diagram of the experimental test arrangement. The testing involved no structural modification of the engine. The engine operated at 2200 rpm, with a gradual increment in the load until the engine speed was reduced to 1000 rpm by steps of 200 rpm. The emissions and EGT were quantified using the Testo 350 analyzer. The dynamometer control panel accurately recorded speed, torque, and momentary fuel consumption. Readings were recorded at a steady state when the engine was stabilized. DF values were used as a reference for other blends. Each test was run three times and the average results were noted.

2.3. Uncertainty analysis

Uncertainty analysis may be used to determine the correctness of established parameters. Furthermore, it shows the amount of inaccuracy in each reading of the experimental setup. Table 6 displays the accuracy, measurable range of parameters, and uncertainty in the measurements. However, the overall uncertainty of the experimental setup (U_{exp}) is estimated using the following equation.

$$U_{exp} = [(U_{power})^2 + (U_{Speed})^2 + (U_{BSFC})^2 + (U_{EGT})^2 + (U_{Nox})^2 + (U_{CO})^2 + (U_{CO2})^2]^{1/2}$$

$$U_{exp} = [(1)^2 + (0.5)^2 + (0.5)^2 + (0.5)^2 + (1)^2 + (1)^2 + (1)^2]^{1/2}$$

$$U_{exp} = 2.18 \%$$

Table 3
Primary parameters of Gas chromatography-flame ionization detection (GC-FID) analysis.

Parameter	Value
Injection Temperature (K)	523
Flow Rate (mL/min)	1.5
Split Ratio	2.1
Carrier Gas	Nitrogen
Oven Program:	
Starting Temperature (K)	423
Hold Time (min)	0.5
Ramp to 473 K (K/min)	35
Ramp to 498 K (K/min)	4
Ramp to 516 K (K/min)	80
Final Hold Time	6

The method and materials utilized to measure the biodiesel's physical characteristics are given in Table 4.

Table 4
Measurement and instrument details for physical characteristics of biodiesel.

Measurement	Instrument/Method Used
Density	VTD-DDM 2911, Temperature Controller: Peltier Thermostat (± 0.01 K)
Viscosity	Rotational Rheometer Temperature Controller: Oil Bath (± 0.3 K)
Iodine Value	EN-16300
CN	Giakoumis and Sarakatsanis Equation
Carbon Residue Content	ASTM-D189-06
Saponification Value	ASTM-D5558-95

Table 5
Technical features of the test engine.

Parameter	Value
Bore(cm)	7.8
Stroke (cm)	6.6
Displacement (cm ³)	315
Injection type	Direct
Maximum Torque(2400 rpm)	15 Nm
Compression ratio	20.3:1
Engine Weight	33 kg
Lubricant Oil Sump Capacity (Liters)	3.1
Recommended Battery	12/144 (V/Ah)

2.4. Optimization of engine operational variables

The study aimed to optimize WCFB proportion and engine speed to achieve optimal performance and emission levels. For this very purpose, RSM was incorporated by using Design Expert-13. RSM aids in effectively exploring the complicated design space and builds a mathematical model using a small number of well-selected experimental points despite evaluating every potential combination of variables [40]. A multi-objective historical design with continuous numeric factors (WCFB proportion and speed) was chosen. Responses included torque, BP BSFC, BTE, CO, CO₂, NOx, and EGT. Optimization was conducted at

95 % confidence interval levels. Experimental interaction between multiple factors was assessed by using Analysis of Variance (ANOVA), a widely used statistical method. The probability that the observed results

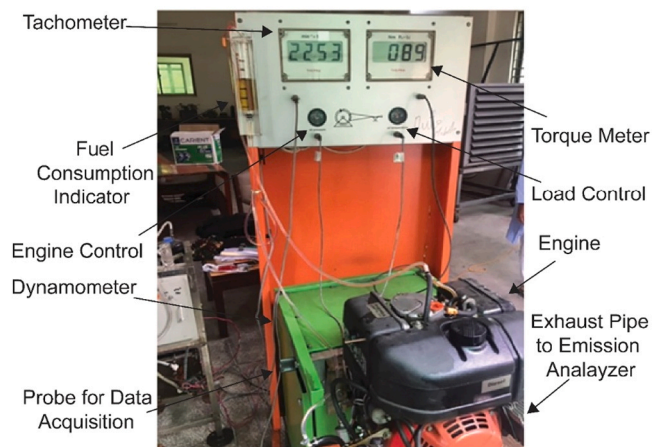


Fig. 2. Original engine test rig.

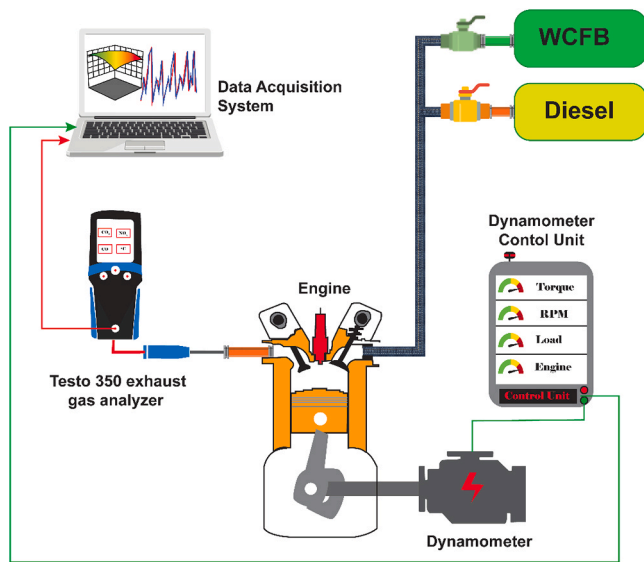


Fig. 3. Schematic diagram of the experimental test arrangement.

Table 6 Accuracy, Measurable range, and Uncertainty in measurements.

Parameters	Range measurable	Accuracy	Uncertainty (%)
Power	0–110 kW	0.5 kW	± 1
Speed	0–7000 rpm	2 rpm	± 0.5
Fuel Consumption	-	0.1 kg/kWh	± 0.5
EGT	0–1300 °C	0.1 °C	± 0.5
NOx	0–4000 ppm	± 5 ppm	± 1
CO	0–10000 ppm	± 10 ppm	± 1
CO ₂	0–50 %	± 0.3 vol%	± 1

Table 7 p-value of the responses obtained by analysis of variance.

Response	A	B	AB
Torque	0.0066	< 0.0001	0.022
BP	0.0204	< 0.0001	0.0091
BSFC	0.0112	< 0.0001	0.0439
BTE	0.00491	< 0.0001	0.0511
CO	0.0257	< 0.0001	0.0002
CO ₂	< 0.0001	< 0.0001	< 0.0001
EGT	0.005	< 0.0001	0.0006
NOx	< 0.0001	< 0.0001	-

A = WCFB Proportion B = Engine Speed

Table 8 Performance matrix of the Response surface methodology (RSM) model.

Response	R ²	Adjusted R ²	Predicted R ²	Lack of fit
Torque	0.9697	0.9484	0.9193	0.0851
BP	0.9839	0.9726	0.9578	0.0924
BSFC	0.9831	0.9712	0.9596	0.2889
BTE	0.9832	0.9715	0.9595	0.1544
CO	0.9731	0.9634	0.9397	0.6409
CO ₂	0.982	0.9789	0.9721	0.7874
EGT	0.9923	0.9896	0.9861	0.9991
NOx	0.9772	0.9758	0.9725	0.0850

might have occurred by chance and that the factor(s) won't significantly affect the response variables was evaluated by p-value. Table 7 illustrates the p-values for the responses below 0.05, suggesting a noteworthy influence of WCFB proportion and engine speed on each response.

The selection of a suitable model relies on the predicted coefficient of determination (R²), a reasonably consistent comparison between the

predicted and adjusted R², and the p-value. An R² value near 1 indicates a perfect linear relationship in the curve. Table 8 displays the R² values obtained from the ANOVA test, which indicate a well-fitting model and strong agreement with the experimental data.

RSM results are interpreted by combining "Weight" and "Importance," which consider data variability and reliability as key factors in distinguishing the response. Table 9 illustrates the limitations and optimization setup. RSM analysis is strengthened by these insights, resulting in increased robustness and effectiveness.

3. Results and discussion

3.1. Methodological advantages of waste chicken fat biodiesel production

In the study, MeOH is injected as microbubbles in the reactor. The minute dimensions and extensive interfacial surfaces of the microbubbles, enhanced mass and heat exchange at the bubble interface. The localized heating from the large heat flux reduced film thickness, promoting faster reaction completion. MeOH microbubbles reduced the buoyancy, prolonging the duration of residence. The reaction starts as the protonated CFO and MeOH bubbles come into contact. Firstly, the process was aided by the abundance of protonated CFO, increasing the concentration of biodiesel. The gradient of CFO concentration lessens over time. Comparing this study to earlier ones, Table 10 demonstrates much better biodiesel conversion in a shorter time.

3.2. Characteristics of chicken fat oil-based biodiesel

The experimentally measured characteristics of CFO-based biodiesels are depicted in Table 11. The calorific value measures significantly higher than the ASTM standard for diesel, indicating its potential as an energy-rich alternative [54]. The carbon residue falls below the EN standard and only slightly exceeds the ASTM standard, positioning it favorably as a substitute for petroleum diesel. Moreover, the CN of CFO-biodiesel surpassed both standards, presenting an attractive alternative fuel choice.

3.3. Performance characteristics

The correlation linking engine speed and braking torque for DF, WCFB10, WCFB20, WCFB30, and WCFB40, is shown in Fig. 4(a). Brake torque increased with engine speed up to 2000 rpm but declined afterward. Despite biodiesel's lower heating values, higher oxygen content enabled greater engine torque at low speeds. This results from enhanced combustion efficiency within the fuel-rich region, effectively harnessing the higher oxygen concentration [28]. Biodiesel blends have higher densities than diesel, leading to more fuel in the cylinder, increasing torque due to viscosity, and reduced pump leakage [55]. The diesel engine power with DF achieved 8.10 Nm torque at 2000 rpm, while WCFB fuels (WCFB10, WCFB20, WCFB30, WCFB40) recorded 8.15 Nm, 8.24 Nm, 8.03 Nm, and 7.99 Nm at the same speed. Comparatively, WCFB20 and WCFB40 showed the highest torque increase, 2.04 %. The torque ratings of biodiesel blends were lower than diesel's above 2000 rpm owing to decreased heating value and high value of viscosity hindering atomization and combustion. Furthermore, the engine encounters constraints in terms of intake airflow, cylinder filling, frictional inefficiencies, valvetrain functioning, exhaust backpressure, and mechanical stress [56].

Fig. 4(b) depicts that when speed increases up to 2000 rpm BP increases. The highest BP achieved by DF was 1696.46 W at 2000 rpm. At the same speed, the BP for WCFB10, WCFB20, WCFB30, and WCFB40 was 1706.93 W, 1725.78 W, 1681.79 W, and 1673.42 W respectively. WCFB20 demonstrated the highest BP among all test fuels.

Fig. 5(a) presents that BSFC first decreases as the engine speed rises until 2000 rpm, after which it declines with higher speeds. Due to increased combustion efficiency and better air-fuel mixing, BSFC

Table 9
Optimization setting of the Response surface methodology (RSM) model.

Variable	Objective	Low Value	High Value	Importance	Low Weight	High Weight
A: WCFB	is in range	0	40	3	1	1
B: RPM	is in range	1000	2200	3	1	1
Torque	maximize	4.82	8.24	3	1	1
BP	maximize	6.99.159	1725.78	3	1	1
BSFC	minimize	0.261	0.551	3	1	1
BTE	maximize	15.24	29.03	3	1	1
CO	minimize	536	725	3	1	1
CO ₂	minimize	2.39	3.77	3	1	1
EGT	minimize	401.45	592.23	3	1	1
NOx	is in range	478	829	3	1	1

Table 10
Comparison of the performance of biodiesel synthesis.

Author	Catalyst	Temperature (°C)	Reaction Time (min)	Conversion (%)
Montefrio et al. [41]	Fe ₂ (SO ₄) ₃	30	1440	45
Tashtoush et al. [42]	H ₂ SO ₄	50	120	78
Elkelawy et al. [43]	TiO ₂	60	60	95
Seffati et al. [44]	CaO/CuFe ₂ O	65	360	92.35
Bhatti et al. [45]	H ₂ SO ₄	50	1440	99.01
Encinar et al. [46]	H ₂ SO ₄	35–65	2880	89
Rad et al. [47]	MWCNT-SO ₃ H	90	600	96.5
Maafa [48]	TPC-SO ₃ H	70	120	98.8
Amal et al. [49]	CaO	65	300	85
Asif et al. [50]	Sr/ZrO ₂	70	20	75
Odetoeye et al. [51]	Egg shell	65	120	90.2
Zhang et al. [52]	Fe ₃ O ₄ @SiO ₂ -SO ₃ H (S)	65	240	97.5
Melero et al. [53]	Zr-SBA-15	209	360	90
Present work	PTSA	70	30	89.9

Table 11
Characteristics comparison of waste chicken fat-based biodiesel.

Properties	EN-14214	ASTM D6751	CFO Biodiesel
FAME (%)	-	-	89.9
FFA (%)	-	-	0.4
Carbon Residue (%)	0.3	0.05	0.0646
Calorific Value (MJ.kg ⁻¹)	-	35	39.98
CN	51	47	52.6
Density (kg.m ⁻³)	860–900 at 20 °C	870–890	895.3
Viscosity (mm ² .sec ⁻¹)	3.50–5.00 at 40 °C	1.90–6.00	4.0654
Saponification Value (mgKOH/g)	Not specified	Not specified	256
Iodine Value	120	Not specified	101.6
Aniline Point (°C)	Not specified	Not specified	68

initially declines (up to 2000 rpm), resulting in lower fuel consumption for a given power output. Beyond 2000 rpm, however, BSFC rises as more fuel is consumed per unit of output due to greater frictional and pumping losses, as well as shorter combustion times, which negate the advantages of enhanced efficiency [57]. The lowest BSFC for DF was recorded to be 0.298 kg/kW.h at 2000 rpm. At the same speed, the BSFC for WCFB10, WCFB20, WCFB30, and WCFB40 was found as 0.2790 kg/kW.h, 0.2610 kg/kW.h, 0.2870 kg/kW.h, and 0.309 kg/kW.h, respectively. WCFB10, WCFB20, and WCFB30 demonstrated a decrease in fuel economy for DF on average of 3.790 %, 6.950 %, and 2.240 % respectively. For WCFB40, BSFC was 2.91 % higher than DF. The high value of density and viscosity of WCFB40 led to delayed pre-mixed combustion due to poor atomization. WCFB20 had the lowermost BSFC at all speeds.

Fig. 5(b) depicts that BTE rises with speed up to a certain point and then declines. This can be credited to higher friction and a reduction in time needed to complete combustion at high engine speeds [58]. DF's highest efficiency of 28.69 % was measured at 2000 rpm. At the same speed, the BTE for WCFB10, WCFB20, WCFB30, and WCFB40 was 28.88 %, 29.03 %, 28.46 %, and 28.21 %, respectively. When compared to DF, the WCFB10 and WCFB20 average increases in BTE were determined as 0.8 %, and 1.9 %, respectively. The average decline in BTE for

WCFB30 and WCFB40 biodiesel blends compared to DF was 1.2 % and 1.9 %, respectively, due to their lower heating values and increased BSFC.

3.4. Analysis of emissions

In Fig. 6(a), as engine speed increases, CO emissions decrease due to the hot cylinder gas accelerating combustion rate [59]. DF exhibited the highest CO emission at 1000 rpm (725 ppm), while WCFB10, WCFB20, WCFB30, and WCFB40 showed lower values at 659 ppm, 647 ppm, 626 ppm, and 614 ppm at the same speed, respectively. Compared to DF, biodiesel blends had average CO emission reductions of 4.04 %, 6.13 %, 7.77 %, and 9.53 %. Higher biodiesel content in diesel blends, along with the presence of oxygen, led to reduced CO emissions.

In Fig. 6(b), CO₂ emissions increase with increasing engine speed for all fuel mixtures. At 2200 rpm, DF exhibited the highest CO₂ emission at 3.77 % vol. The biodiesel blends (WCFB10, WCFB20, WCFB30, and WCFB40) had lower CO₂ emissions: 3.68 % V, 3.62 % V, 3.58 % V, and 3.49 % V, respectively. The oxygen content in biodiesel results in a gradual CO₂ increase with increasing fuel quantity in comparison to diesel [60]. The average CO₂ reductions for WCFB10, WCFB20, WCFB30, and WCFB40 compared to diesel were 2.36 %, 4.84 %, 7.51 %, and 11.88 %, respectively.

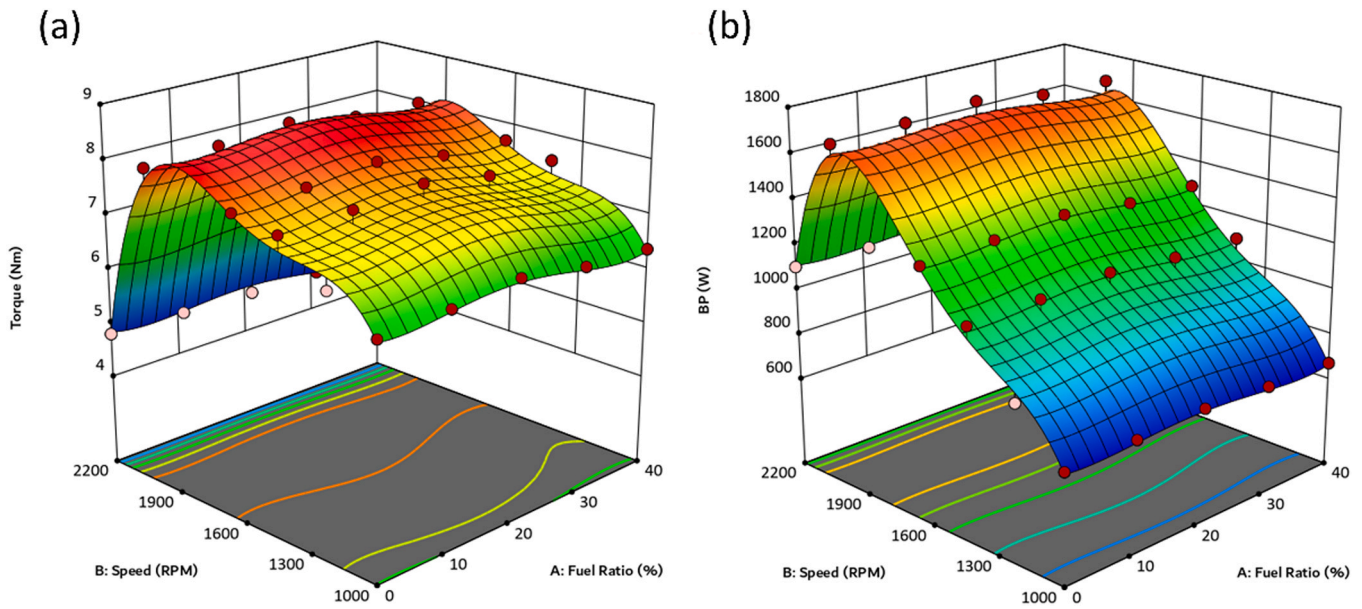


Fig. 4. Surface plot for (a) torque, and (b) brake power.

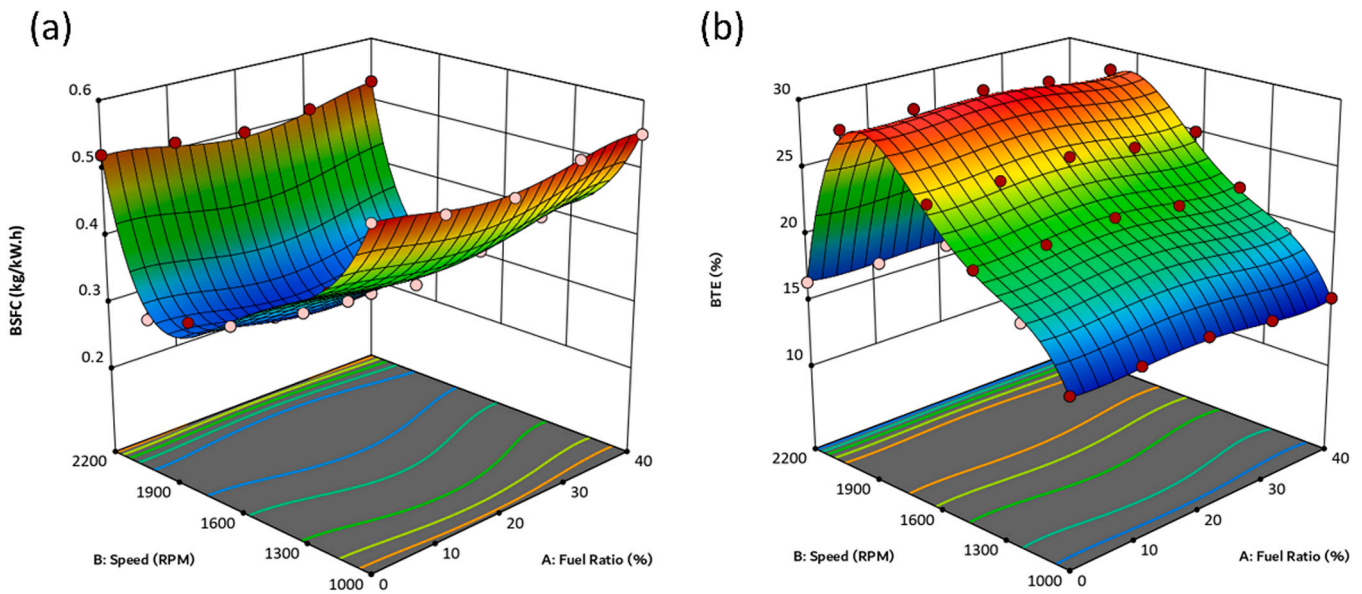


Fig. 5. Surface plot for the analysis of (a) brake-specific fuel consumption, and (b) brake thermal efficiency.

In Fig. 7(a), the EGT rises with engine speed, primarily because of the rate of combustion and lower heating values of biodiesel blends, causing delayed ignition and increased cylinder pressure and combustion temperature [61]. The highest exhaust gas temperature achieved by diesel was 509.45 K at 2200 rpm. For biodiesel blends WCFB10, WCFB20, WCFB30, and WCFB40, the highest temperatures were 552.45 K, 579.78 K, 585 K, and 592.23 K respectively at 2200 rpm. The average temperature increase compared to diesel was 8.98 %, 10.84 %, 12.02 %, and 13.12 % respectively.

Fig. 7(b) illustrates that NOx emissions increase with higher amounts of biodiesel mixed with DF. The elevated exhaust gas temperature resulting from the biodiesel blends' higher oxygen content is responsible for the rise in NOx emission. At 2200 rpm, NOx emissions using pure diesel were 801.9 ppm, while they were 804 ppm, 810 ppm, 818 ppm, and 829 ppm for WCFB10, WCFB20, WCFB30, and WCFB40, respectively. Compared to diesel, the average NOx emission increases were 2.750 %, 4.90 %, 7.650 %, and 10.690 % for WCFB10, WCFB20,

WCFB30, and WCFB40, respectively. The elevated combustion temperature and extended ignition delay resulting from the reduced heating value and elevated oxygen content present in biodiesel led to increased NOx emissions during the premixed combustion phase.

3.5. Engine optimization results

The ramp chart in Fig. 8 presents the optimization results. The optimization aimed to maximize BP and BTE while minimizing BSFC, CO, CO₂, and NOx. The 14.2 % volume percentage of WCFB and 1845.3 rpm were found to be the engine's optimized operating parameters. With a torque of 8.4 Nm, BP of 1632.1 W, BSFC of 0.27 kg/kW.h, BTE of 28.9 %, and low emissions of CO (570.7 ppm), CO₂ (3.50 %V), EGT of 544.3 K, and NOx (710.7 ppm), the engine displayed advantageous performance and emission characteristics at these settings. A comparison of optimized results with DF is presented in Table 12. The negative symbol implies a percentage decline. The optimized model is

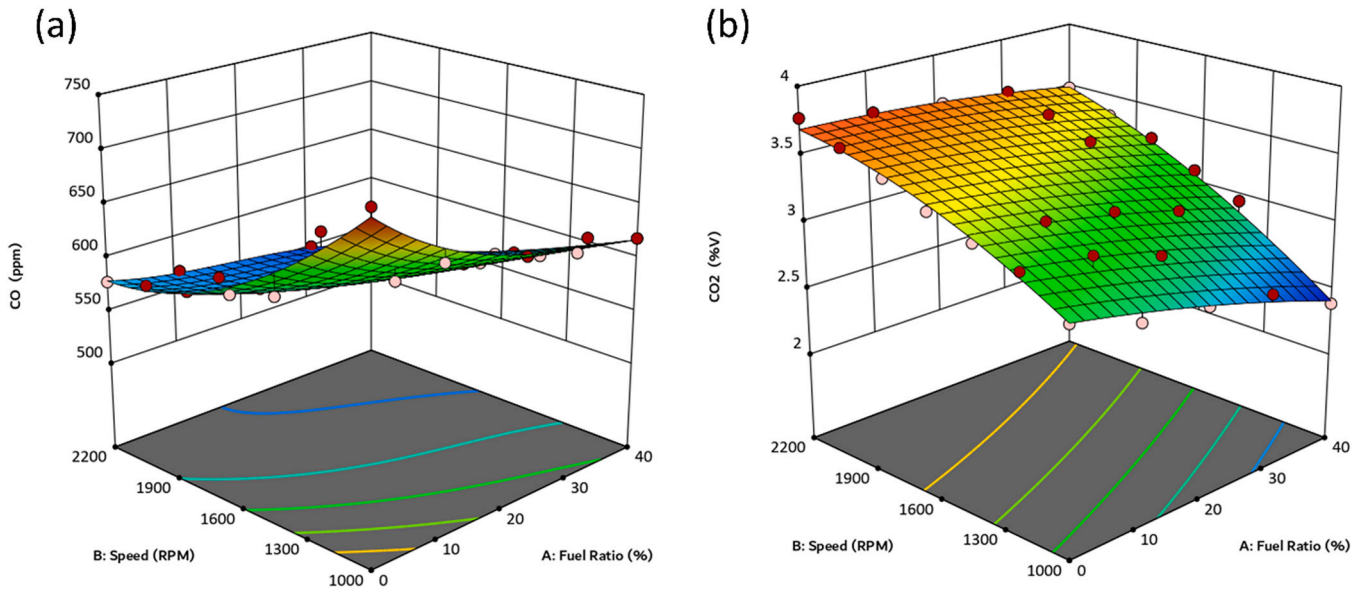


Fig. 6. Surface plot for the analysis of (a) carbon monoxide, and (b) carbon dioxide.

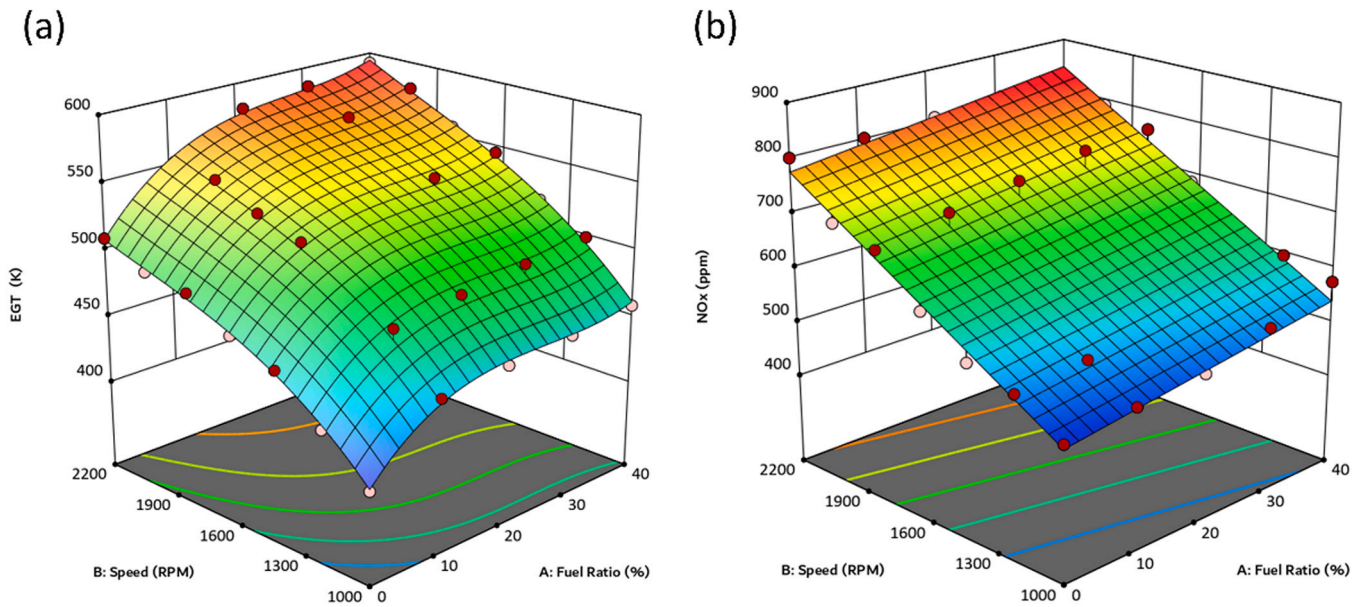


Fig. 7. Surface plot for the analysis of (a) emission gas temperature, and (b) nitrogen oxides.

validated by the derived composite desirability (D) value of 0.790, which shows that the engine responses have been effectively optimized. The outcomes are in line with the study’s goals. The results of the confirmation test that was conducted to experimentally verify the optimized results are presented in Table 13. Acceptable percentage error confirms the effectiveness of the RSM model.

4. Conclusion and outlook

Microbubbles speed up the infusion of methanol during single-step esterification with PTSA as a catalyst, substantially slashing the time of reaction from hours to minutes. This increases WCFB production feasibility significantly and improves conversion rates and production economics. The characteristics comparison of WCFB indicates that it can be employed as an alternative to DF. The current research is confined to the optimization of engine parameters using RSM. However, future research should focus on intricate transesterification in biodiesel

production, considering factors like temperature, time, and catalysts. Precise modeling through machine learning techniques like ANN is crucial for efficiency, quality, and cost reduction.

RSM model with a composite desirability value of 0.790 determined the engine’s optimized parameters to be a WCFB volume fraction of 14.2 % and an engine speed of 1845.3 rpm. When compared to DF powered engine, the results were in line with the study goals. Torque, BP, and BTE increased by 5.6 %, 8.9 %, and 7.7 %, respectively. A 15.9 % reduction is observed in BSFC. Additionally, CO emissions decreased by 4.6 %. Higher levels of oxygen and hydrogen in the mixture boosted combustion, which increased heat production and raised the temperatures of the exhaust gases. Therefore 10.9 % and 4 % increases in EGT and NOx emissions respectively were observed. The error percentage of the confirmation test was within the limit of 5 % which affirmed the robustness of the RSM model for optimization.

The study provides a solid framework for future-centered efforts aligned with SGDs 7, 12, 13, and 17. Industrial-scale WCFB production

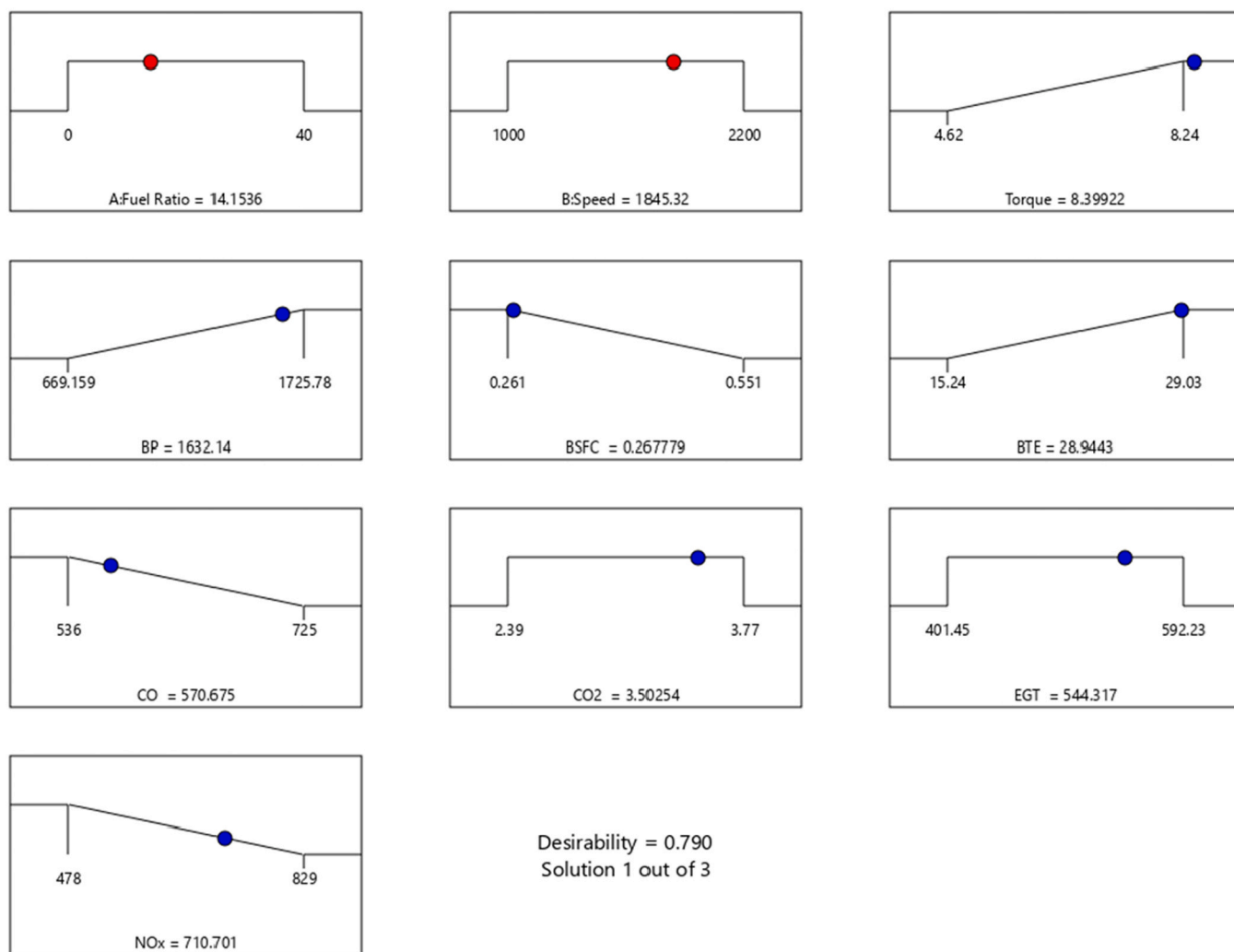


Fig. 8. Ramp chart of the Response surface methodology (RSM) model showing optimized results.

Table 12

Examining outputs at optimal operating conditions relative to pure diesel fuel.

Fuel Ratio	Speed (rpm)	Torque (Nm)	BP (W)	BSFC (kg/kW.h)	BTE (%)	CO (ppm)	CO ₂ (% V)	EGT (K)	NO _x (ppm)
14.2	1845.3	8.4	1632.1	0.27	28.9	570.7	3.50	544.3	710.7
0.0	1845	8.0	1498.5	0.32	26.9	598.0	3.53	491.0	689.0
Difference (%)		5.6	8.9	-15.9	7.7	-4.6	-0.8	10.9	3.1

Table 13

Outcomes drawn from the verification of the test.

	Torque	BP	BTE	BSFC	CO	CO ₂	HC	NO _x
Optimized Value	8.4	1632.1	0.27	28.9	570.7	3.50	544.3	710.7
Test Value	8.7	1664.4	0.26	29.8	594.1	3.64	520.4	682.3
Error (%)	3.2	3.1	3.6	3.0	4.1	3.9	4.4	4.0

minimizes waste, and generates renewable energy, and waste-to-energy integration addresses holistic waste management and energy needs. Future research should expand on the sustainability implications of the current findings by employing advanced sustainability assessment tools, including Life Cycle Assessment (LCA), exergy analysis, and energy analysis, among others. The methodologies enable a holistic evaluation of environmental, economic, and energy-based impacts across the entire production lifecycle. Applying these methods to biodiesel systems, for

example, can offer insights into resource use efficiency, emissions, waste generation, and overall environmental impact. Integrating these advanced sustainability assessments is crucial for identifying potential areas for improvement in biofuel production and optimizing bioenergy systems. This direction not only allows researchers to gauge the broader impact of biodiesel production on ecological and economic systems but also informs regulatory and policy decisions, supporting the development of more sustainable biofuel solutions. Such assessments will guide

future studies toward processes that enhance sustainability, reducing carbon footprints, and minimizing ecological disruption. Additionally, integrating Waste chicken fat biodiesel (WCFB) into wider bioenergy and bioproduct systems should be explored to understand synergies and trade-offs among renewable technologies, offering a holistic view of sustainability and economic potential.

Nomenclature

BTE: Brake thermal efficiency
 BP: Brake power
 BSFC: Brake-specific fuel consumption
 CFO: Chicken fat oil
 CN: Cetane Number
 DF: Diesel fuel
 EGT: Exhaust gas temperature
 FAMES: Fatty acid methyl esters
 FFAs: Free fatty acids
 HC: Hydrocarbons
 ICEs: Internal combustion engines
 PTSA: P-toluene sulfonic acid
 SDGs: Sustainable development goals
 VTD: Vibrating tube densitometer
 WCF: Waste chicken fat
 WCFB: Waste chicken fat biodiesel

CRedit authorship contribution statement

Yasser Fouad: Funding acquisition, Resources, Writing – review & editing. **Fahed Javed:** Resources, Software, Writing – review & editing. **M.A. Mujtaba:** Data curation, Investigation, Visualization. **M.A. Kalam:** Methodology, Project administration, Writing – review & editing. **Muhammad Usman:** Conceptualization, Methodology, Writing – original draft. **Muhammad Abrar:** Investigation, Methodology. **Touqeer Ahmad:** Formal analysis, Software. **Fahid Riaz:** Data curation, Formal analysis, Funding acquisition. **Fahad Rehman:** Validation, Writing – review & editing. **Nasir Hayat:** Conceptualization, Supervision, Visualization.

Conflict of interest

The author on the behalf of the all other authors, declare that there is no conflict of interest and all the elements of the submission are also in compliance with the journal publishing ethics. By submitting this manuscript, the authors agreed that the copyright for their article should be transferred to this journal if the article is accepted for publication. The work contained within the research paper is our original contribution and has not been published anywhere.

Declaration of Competing Interest

The authors declare that they have no known competing financial interests or personal relationships that could have appeared to influence the work reported in this paper.

Acknowledgments

The authors extend their appreciation to the Researchers Supporting Project number (RSPD2025R698), King Saud University, Riyadh, Saudi Arabia for funding this research work.

Also, the authors acknowledge the support and facilities provided by the University of Engineering and Technology, Lahore-Pakistan.

References

- [1] G. Kalghatgi, Is it really the end of internal combustion engines and petroleum in transport? *Appl. Energy* 225 (2018) 965–974, <https://doi.org/10.1016/j.apenergy.2018.05.076>.
- [2] L. Lešnik, et al., Why we should invest further in the development of internal combustion engines for road applications, *Oil Gas. Sci. Technol. Rev. d'IFP Energ. Nouv.* 75 (2020) 56, <https://doi.org/10.2516/ogst/2020051>.
- [3] A.S. Badday, et al., Intensification of biodiesel production via ultrasonic-assisted process: a critical review on fundamentals and recent development, *Renew. Sustain. Energy Rev.* 16 (7) (2012) 4574–4587, <https://doi.org/10.1016/j.rser.2012.04.057>.
- [4] T. Michael, Environmental and social impacts of waste to energy (WTE) conversion plants. *Waste to Energy Conversion Technology*, Elsevier, 2013, pp. 15–28, <https://doi.org/10.1533/9780857096364.1.15>.
- [5] L. Montanarella, R. Vargas, Global governance of soil resources as a necessary condition for sustainable development, *Curr. Opin. Environ. Sustain.* 4 (5) (2012) 559–564, <https://doi.org/10.1016/j.cosust.2012.06.007>.
- [6] R. Luque, et al., Biodiesel as feasible petrol fuel replacement: a multidisciplinary overview, *Energy Environ. Sci.* 3 (11) (2010) 1706–1721, <https://doi.org/10.1039/C0EE00085J>.
- [7] M.P. Sudeshkumar, et al., Waste plastic oil to fuel: An experimental study in thermal barrier coated CI engine with exhaust gas recirculation, *Environ. Qual. Manag.* 32 (1) (2022) 125–131, <https://doi.org/10.1002/tqem.21853>.
- [8] N. Khan, K. Sudhakar, R. Mamat, Thermogravimetric analysis of marine macroalgae waste biomass as bio-renewable fuel, *J. Chem.* 2022 (2022), <https://doi.org/10.1155/2022/6417326>.
- [9] E. Alptekin, M. Canakci, Optimization of transesterification for methyl ester production from chicken fat, *Fuel* 90 (8) (2011) 2630–2638, <https://doi.org/10.1016/j.fuel.2011.03.042>.
- [10] M. Arshad, et al., Electricity generation from biogas of poultry waste: an assessment of potential and feasibility in Pakistan, *Renew. Sustain. Energy Rev.* 81 (2018) 1241–1246, <https://doi.org/10.1016/j.rser.2017.09.007>.
- [11] A. Abedullah, A. Maqbool, K. Bukhsh, Issues and economics of poultry production: a case study of Faisalabad, *Pakistan, Pak. Vet. J.* 27 (1) (2007) 25–28, 26520417.
- [12] J. Wang, et al., Intensifying biofuel production using a novel bionic flow-induced peristaltic reactor: biodiesel production as a case study, *Biofuel Res. J.* 9 (4) (2022) 1721–1735.
- [13] M. Kirubakaran, V.A.M. Selvan, A comprehensive review of low cost biodiesel production from waste chicken fat, *Renew. Sustain. Energy Rev.* 82 (2018) 390–401, <https://doi.org/10.1016/j.rser.2017.09.039>.
- [14] S. Kumar, N. Kumar, S. Vivekadhish, Millennium development goals (MDGs) to sustainable development goals (SDGs): addressing unfinished agenda and strengthening sustainable development and partnership, *Indian J. Community Med.: Off. Publ. Indian Assoc. Prev. Soc. Med.* 41 (1) (2016) 1, <https://doi.org/10.4103/0970-0218.170955>.
- [15] M. Elkelawy, et al., Study of performance, combustion, and emissions parameters of DI-diesel engine fueled with algae biodiesel/diesel/n-pentane blends, *Energy Convers. Manag.*: X 10 (2021) 100058, <https://doi.org/10.1016/j.ecmx.2020.100058>.
- [16] M.N. Abdullah, et al., Sustainable biofuels from first three alcohol families: a critical review, *Energies* 16 (2) (2023) 648, <https://doi.org/10.3390/en16020648>.
- [17] W. Shi, et al., Biodiesel production from waste chicken fat with low free fatty acids by an integrated catalytic process of composite membrane and sodium methoxide, *Bioresour. Technol.* 139 (2013) 316–322, <https://doi.org/10.1016/j.biortech.2013.04.040>.
- [18] A. Talebian-Kiakalaieh, N.A.S. Amin, H. Mazaheri, A review on novel processes of biodiesel production from waste cooking oil, *Appl. Energy* 104 (2013) 683–710, <https://doi.org/10.1016/j.apenergy.2012.11.061>.
- [19] M. Zheng, et al., Biodiesel engine performance and emissions in low temperature combustion, *Fuel* 87 (6) (2008) 714–722, <https://doi.org/10.1016/j.fuel.2007.05.039>.
- [20] L. Wei, C.S. Cheung, Z. Ning, Effects of biodiesel-ethanol and biodiesel-butanol blends on the combustion, performance and emissions of a diesel engine, *Energy* 155 (2018) 957–970, <https://doi.org/10.1016/j.energy.2018.05.049>.
- [21] R. Behçet, et al., Comparison of exhaust emissions of biodiesel–diesel fuel blends produced from animal fats, *Renew. Sustain. Energy Rev.* 46 (2015) 157–165, <https://doi.org/10.1016/j.rser.2015.02.015>.
- [22] A.S. El-Shafay, et al., Waste to energy: Production of poultry-based fat biodiesel and experimental assessment of its usability on engine behaviors, *Energy* 262 (2023) 125457, <https://doi.org/10.1016/j.energy.2022.125457>.
- [23] T. Shudo, et al., The cold flow performance and the combustion characteristics with ethanol blended biodiesel fuel, *SAE Tech. Paper* (2005), <https://doi.org/10.4271/2005-01-3707>.
- [24] V. Dhana Raju, et al., Experimental assessment of diverse diesel engine characteristics fueled with an oxygenated fuel added lemon peel biodiesel blends, *Fuel* 324 (2022) 124529, <https://doi.org/10.1016/j.fuel.2022.124529>.
- [25] H. Aydin, C. Ilkılıç, Effect of ethanol blending with biodiesel on engine performance and exhaust emissions in a CI engine, *Appl. Therm. Eng.* 30 (10) (2010) 1199–1204, <https://doi.org/10.1016/j.applthermaleng.2010.01.037>.
- [26] P.K. Chaurasiya, et al., Influence of injection timing on performance, combustion and emission characteristics of a diesel engine running on hydrogen-diethyl ether, n-butanol and biodiesel blends, *Int. J. Hydrog. Energy* 47 (41) (2022) 18182–18193, <https://doi.org/10.1016/j.ijhydene.2022.03.268>.
- [27] M. Elkelawy, et al., Maximization of biodiesel production from sunflower and soybean oils and prediction of diesel engine performance and emission

- characteristics through response surface methodology, *Fuel* 266 (2020) 117072, <https://doi.org/10.1016/j.fuel.2020.117072>.
- [28] U. Rajak, et al., Numerical analysis of performance and emission behavior of CI engine fueled with microalgae biodiesel blend, *Mater. Today.: Proc.* 49 (2021), <https://doi.org/10.1016/j.matpr.2021.02.104>.
- [29] D. Barik, R. Vijayaraghavan, Effects of waste chicken fat derived biodiesel on the performance and emission characteristics of a compression ignition engine, *Int. J. Ambient Energy* 41 (1) (2020) 88–97, <https://doi.org/10.1080/01430750.2018.1451370>.
- [30] M.N. Mohiddin, et al., A study on chicken fat as an alternative feedstock: biodiesel production, fuel characterisation, and diesel engine performance analysis, *Int. J. Automot. Mech. Eng.* 15 (3) (2018) 5535–5546, <https://doi.org/10.15282/ijame.15.3.2018.10.0425>.
- [31] M. Kirubakaran, Eggshell as heterogeneous catalyst for synthesis of biodiesel from high free fatty acid chicken fat and its working characteristics on a CI engine, *J. Environ. Chem. Eng.* 6 (4) (2018) 4490–4503, <https://doi.org/10.1016/j.jece.2018.06.027>.
- [32] M. Şen, A.O. Emiroğlu, A. Keskin, Production of biodiesel from broiler chicken rendering fat and investigation of its effects on combustion, performance, and emissions of a diesel engine, *Energy Fuels* 32 (4) (2018) 5209–5217, <https://doi.org/10.1021/acs.energyfuels.8b00278>.
- [33] L. Yi-Chia, et al., Role of chicken fat waste and hydrogen energy ratio as the potential alternate fuel with nano-additives: insights into resources and atmospheric remediation process, *Environ. Res.* 216 (2023) 114742, <https://doi.org/10.1016/j.envres.2022.114742>.
- [34] C. Wang, et al., Comparative assessment of waste cooking, chicken waste and waste tire biodiesel blends on performance and emission characteristics, *Fuel* 320 (2022) 123859, <https://doi.org/10.1016/j.fuel.2022.123859>.
- [35] N. Kinnal, et al., Investigation on performance of diesel engine by using waste chicken fat biodiesel, in *IOP Conference Series: Materials Science and Engineering*, IOP Publishing, 2018, <https://doi.org/10.1088/1757-899X/376/1/012012>.
- [36] W.B. Zimmerman, M.K. Al-Mashhadani, H.H. Bandulasena, Evaporation dynamics of microbubbles, *Chem. Eng. Sci.* 101 (2013) 865–877, <https://doi.org/10.1016/j.ces.2013.05.026>.
- [37] W.B.J. Zimmerman, V. Tesar, Bubble generation for aeration and other purposes, *Google Pat.* (2012), <https://doi.org/10.1016/j.cherd.2017.01.034>.
- [38] W.B. Zimmerman, R. Kokoo, Esterification for biodiesel production with a phantom catalyst: bubble mediated reactive distillation, *Appl. Energy* 221 (2018) 28–40, <https://doi.org/10.1016/j.apenergy.2018.03.147>.
- [39] F. Javed, et al., Conversion of poultry-fat waste to a sustainable feedstock for biodiesel production via microbubble injection of reagent vapor, *J. Clean. Prod.* 311 (2021) 127525, <https://doi.org/10.1016/j.jclepro.2021.127525>.
- [40] P. Sharma, et al., Exploring the exhaust emission and efficiency of algal biodiesel powered compression ignition engine: application of box–behnen and desirability based multi-objective response surface methodology, *Energies* 14 (18) (2021) 5968, <https://doi.org/10.3390/en14185968>.
- [41] M.J. Montefrio, T. Xinwen, J.P. Obbard, Recovery and pre-treatment of fats, oil and grease from grease interceptors for biodiesel production, *Appl. Energy* 87 (10) (2010) 3155–3161, <https://doi.org/10.1016/j.apenergy.2010.04.011>.
- [42] G.M. Tashtoush, M.I. Al-Widyan, M.M. Al-Jarrah, Experimental study on evaluation and optimization of conversion of waste animal fat into biodiesel, *Energy Convers. Manag.* 45 (17) (2004) 2697–2711, <https://doi.org/10.1016/j.enconman.2003.12.009>.
- [43] M. Elkelawy, et al., WCO biodiesel production by heterogeneous catalyst and using cadmium (II)-based supramolecular coordination polymer additives to improve diesel/biodiesel fueled engine performance and emissions, *J. Therm. Anal.* Calorim. 147 (11) (2022) 6375–6391, <https://doi.org/10.1007/s10973-021-10920-1>.
- [44] K. Seffati, et al., Enhanced biodiesel production from chicken fat using CaO/CuFe₂O₄ nanocatalyst and its combination with diesel to improve fuel properties, *Fuel* 235 (2019) 1238–1244, <https://doi.org/10.1016/j.fuel.2018.08.118>.
- [45] H.N. Bhatti, M.A. Hanif, M. Qasim, Biodiesel production from waste tallow, *Fuel* 87 (13–14) (2008) 2961–2966, <https://doi.org/10.1016/j.fuel.2008.04.016>.
- [46] J. Encinar, et al., Study of biodiesel production from animal fats with high free fatty acid content, *Bioresour. Technol.* 102 (23) (2011) 10907–10914, <https://doi.org/10.1016/j.biortech.2011.09.068>.
- [47] Rad, A.S., et al., Esterification of waste chicken fat: sulfonated MWCNT toward biodiesel production. *Waste and biomass valorization*, 2018. 9: p. 591–599. DOI: 10.13005/bbra/2279.
- [48] I.M. Maafa, Biodiesel synthesis from high free-fatty-acid chicken fat using a scrap-tire derived solid acid catalyst and KOH, *Polymers* 14 (3) (2022) 643.
- [49] R. Amal, et al., An insight into the catalytic properties and process optimization of Fe, Ni doped eggshell derived CaO for a green biodiesel synthesis from waste chicken fat, *Catal. Commun.* 187 (2024) 106848, <https://doi.org/10.1016/j.catcom.2024.106848>.
- [50] M. Asif, et al., Investigating biodiesel production from Chicken fat oil using bi-functional catalysts and microbubble mediated mass transfer, *Fuel* 358 (2024) 130125, <https://doi.org/10.1016/j.fuel.2023.130125>.
- [51] T.E. Odetoye, J.O. Agu, E.O. Ajala, Biodiesel production from poultry wastes: waste chicken fat and eggshell, *J. Environ. Chem. Eng.* 9 (4) (2021) 105654, <https://doi.org/10.1016/j.jece.2021.105654>.
- [52] H. Zhang, et al., Catalytic high-yield biodiesel production from fatty acids and non-food oils over a magnetically separable acid nanosphere, *Ind. Crops Prod.* 173 (2021) 114126, <https://doi.org/10.1016/j.indcrop.2021.114126>.
- [53] J.A. Meleró, et al., Zr-SBA-15 acid catalyst: optimization of the synthesis and reaction conditions for biodiesel production from low-grade oils and fats, *Catal. Today* 195 (1) (2012) 44–53, <https://doi.org/10.1016/j.cattod.2012.04.025>.
- [54] S. Chandra Sekhar, et al., Biodiesel production process optimization from *Pithecellobium dulce* seed oil: Performance, combustion, and emission analysis on compression ignition engine fuelled with diesel/biodiesel blends, *Energy Convers. Manag.* 161 (2018) 141–154, <https://doi.org/10.1016/j.enconman.2018.01.074>.
- [55] H. An, et al., Combustion and emissions characteristics of diesel engine fueled by biodiesel at partial load conditions, *Appl. Energy* 99 (2012) 363–371, <https://doi.org/10.1016/j.apenergy.2012.05.049>.
- [56] A.A. Al-Kheraif, et al., Experimental assessment of performance, combustion and emission characteristics of diesel engine fuelled by combined non-edible blends with nanoparticles, *Fuel* 295 (2021) 120590, <https://doi.org/10.1016/j.fuel.2021.120590>.
- [57] H. Saleh, Effect of exhaust gas recirculation on diesel engine nitrogen oxide reduction operating with jojoba methyl ester, *Renew. Energy* 34 (10) (2009) 2178–2186, <https://doi.org/10.1016/j.renene.2009.03.024>.
- [58] V. Hariram, G.M. Kumar, Combustion analysis of algal oil methyl ester in a direct injection compression ignition engine, *J. Eng. Sci. Technol.* 8 (1) (2013) 77–92.
- [59] V. Hariram, G.M. Kumar, Combustion analysis of algal oil methyl ester in a direct injection compression ignition engine, *J. Eng. Sci. Technol.* 8 (1) (2013) 77–92.
- [60] C.-Y. Lin, R.-J. Li, Engine performance and emission characteristics of marine fish-oil biodiesel produced from the discarded parts of marine fish, *Fuel Process. Technol.* 90 (7–8) (2009) 883–888, <https://doi.org/10.1016/j.fuproc.2009.04.009>.
- [61] J. Xue, Combustion characteristics, engine performances and emissions of waste edible oil biodiesel in diesel engine, *Renew. Sustain. Energy Rev.* 23 (2013) 350–365, <https://doi.org/10.1016/j.rser.2013.02.039>.